Journal of Medicinal Chemistry

BRIEF ARTICLE

pubs.acs.org/jmc

Preparation and Characterization of Amino-Linked Heterocyclic Carbene Palladium, Gold, and Silver Complexes and Their Use as Anticancer Agents That Act by Triggering Apoptotic Cell Death

Chie-Hong Wang,[†,‡] Wei-Chih Shih,[†] Hui Chuan Chang,[†] Yi-Yin Kuo,[†] Wen-Chun Hung,[‡] Tiow-Gan Ong,[*,†] and Wen-Shan Li[*,†]

[†]Institute of Chemistry, Academia Sinica, Taipei 115, Taiwan

[‡]Institute of Biomedical Sciences, National Sun Yat-Sen University, Kaohsiung 804, Taiwan

Supporting Information

ABSTRACT: Transition metal complexes bearing amino linked N-heterocyclic carbenes (NHC) were prepared and evaluated for their antiproliferative activities in human cancer cells. The optimum antiproliferative activity, observed for the gold complex **3** in U-87 MG cells, was found to involve S-phase arrest of the cell cycle. The results indicate that **3** induces apoptosis through a p53-bak pathway, a finding that could serve as a new strategy to reduce the resistance of cancer cells to p53-induced apoptosis.

INTRODUCTION

The remarkable discovery that N-heterocyclic carbenes (NHCs) serve as neutral σ-donating ligand platforms quickly prompted significant breakthroughs in homogeneous transition metal catalysis.[1] In contrast, biomedical applications of metal NHC complexes have developed only slowly.[2] More recently, hybrid ligand sets developed by Arnold and Fryzuk, in which amine functional groups are linked to NHC, have begun to receive great attention.[3] Interest in these ligands is a result of the fact that they simultaneously utilize an anionic σ-amine group and a neutral, strongly electron donating NHC scaffold to provide stability for hard electropositive metal centers. In addition, libraries of these ligands can be prepared in a relatively straightforward manner. Despite these properties, the biological consequences of these unique molecular motifs remain understudied.

Driven by the desire to uncover new metal complexes that catalyze tumor degradation, a study has been conducted to prepare amino-NHC complexes of Au, Ag, and Pd and to probe their cytotoxic effects in three human cancer cell lines including MCF7, MDA-MB-231 (breast adenocarcinoma), and U-87 MG (glioblastoma). The results of this effort described below show that a gold complex **3** has optimum antiproliferative activity in U-87 MG human glioblastoma cells and that this activity involves S-phase arrest of the cell cycle with a distinctive decrease in the expression of cyclin A, cyclin B, and cyclin-dependent kinase 2. In addition, observations indicate that **3** induces apoptosis through externalization of membrane phosphatidylserine, DNA fragmentation, poly(ADP-ribose)polymerase cleavage, and activation of caspase-3.

RESULT AND DISCUSSION

The respective palladium and gold complexes **2** and **3**, bearing an amino-NHC ligand, were prepared in satisfactory yields through reactions of free amino-NHC **1** with $[(C_3H_5)PdCl]_2$ and AuCl (Scheme 1). In contrast, the amino-NHC AgBr complex **4** was synthesized by reacting Ag_2O with the imidazolium salt of **1**. Single crystal X-ray diffraction analysis of **2** (Figure 1b, top) showed that its cationic palladium is coordinated to the allylic fragment in a η3 manner and to C(7) and N(1) sites of the amino-NHC ligand. The observed Pd−C (carbene) bond distance of 2.014(3) Å is in excellent agreement with those reported earlier for similar substances.[4] Crystal structural analysis shows that in contrast to its Pd counterpart, gold complex **3** contains an essentially linear (177.4°) two-coordinated gold(I) C(7)−Au−Cl(1) arangement (Figure 1b, bottom).[5] The compositions and identities of complexes **2**, **3**, and **4**, characterized by using NMR spectroscopy and elemental analysis, were found to be in complete accord with those arising from X-ray crystallographic studies.

The pharmacological properties of metallodrugs are normally governed by the metal and auxiliary ligand(s).[2b,6] In principle, the lipophilicity and reactivity of metal complexes can be tuned systematically by varying the ligand. We postulated that the lipophilic mesityl group embedded in ligand **1** would enable cell penetration and hence would be effective in delivering an active metal warhead to cancer cell targets. To assess the pharmacokinetic properties of the amino-NHC metal complexes **2**−**4** with respect to the reference drug cisplatin, growth inhibition assays were carried out using three different human cancer cell lines, including breast adenocarcinoma (MCF 7 and MDA-MB-231) and glioblastoma (U-87 MG) (Table 1). Interestingly, in contrast to the Ag complex **4** the Pd and Au complexes **2** and **3** display greater antiproliferative activities than cisplatin against all of the human cancer cell lines. The palladium complex **2** has an IC_{50} of 4.50 μM in MDA-MB-231 cells, a value that is 3-fold lower than that of gold complex **3** (14.22 μM) and approximately

Received: August 24, 2010
Published: June 14, 2011

Scheme 1. Synthetic Route for Complexes 2−4

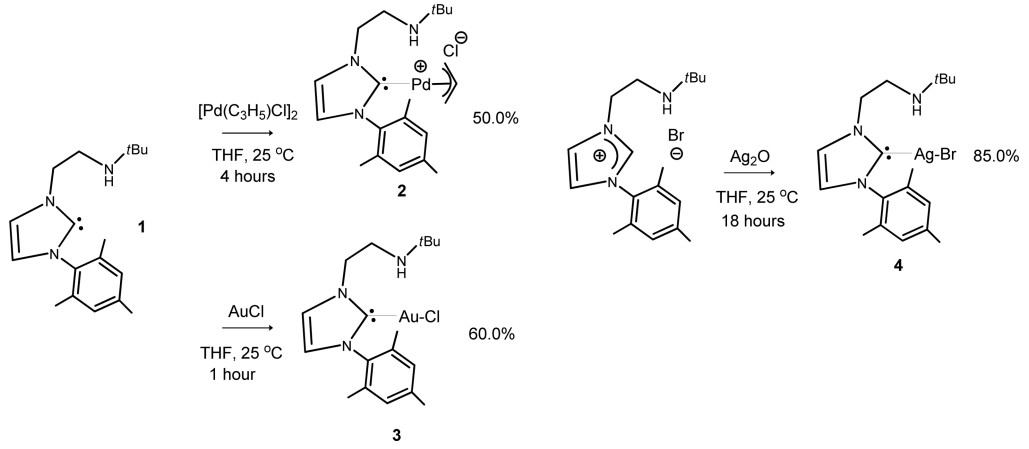

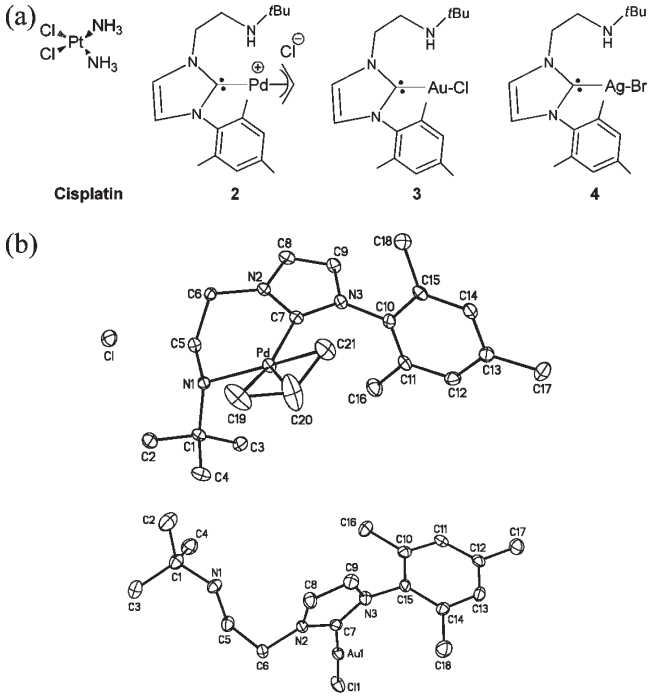

Figure 1. (a) Structures of cisplatin and metal NHC complexes **2**−**4** used in this study. (b) Molecular diagram of **2** (top) and **3** (bottom) with thermal ellipsoids drawn at the 30% probability level. Hydrogen atoms are omitted for clarity.

10-fold lower than that of Ag complex **4** (46.58 μM) and cisplatin (48.43 μM). This finding demonstrates that the anticancer activities of the amino-NHC metal complexes are not solely dependent on molecular hydrophobicity and that activities can be altered by the choice of the metal ion. Significantly, the relative IC_{50} values of **2** and **3** display similar trends in the ER+ cell line MCF-7 and ER− cell line MDA-MB-231, an observation that suggests that the effects on cell viability might be caused by an ER-independent pathway. Overall, the potency order for growth inhibition of breast cancer cells by these complexes was found to be Pd > Au > Ag. In comparison to its palladium counterpart gold complex **3** exhibits a high potency and cellular selectivity toward U-87 MG glioblastoma cells (1.26 μM).

Table 1. In Vitro Cell Viability Effects of Metal NHC Complexes 2−4 Compared to Cisplatin

	IC_{50} (μM)[a]		
compd	MCF-7	MDA-MB-231	U-87 MG
cisplatin	25.81 ± 0.65	48.43 ± 2.67	8.22 ± 0.37
2	6.47 ± 0.07	4.50 ± 0.07	10.25 ± 0.46
3	16.28 ± 0.49	14.22 ± 0.16	1.26 ± 0.04
4	28.68 ± 0.69	46.58 ± 2.13	25.24 ± 0.21

[a] Amount of drug and metal NHC complexes necessary to inhibit the growth of breast (MCF-7/MDA-MB-231) and glioblastoma cells (U-87 MG) by 50% in 48 h. Data are the mean ± SD (n = 3).

A greater understanding of the mechanism of the growth inhibitory effects of metal complex **3** should aid in the design of more effective anticancer therapeutic agents. As a result, studies were carried out to explore alterations that occur in cell cycle progression as a consequence of inhibition of glioblastoma cell proliferation. For this purpose, U-87 MG cells were incubated in the absence and presence of **3** (1.5 and 3.0 μM) for 48 h prior to cell cycle distribution analysis using flow cytometry. The analysis of U-87 MG cells indicates that a significant decrease takes place in the G_1-phase with a concomitant accumulation in S-phase cells and a minor increase in the sub-G_1 population (Figure 2), signaling S-phase arrest. Next, U-87 MG cells were pretreated with complex **3** and pulse-labeled with BrdU before sorting by using FACS analysis. Complex **3** at 2 μM was found to suppress 40% of BrdU uptake throughout S-phase arrest over a period of 24 h (Supporting Information Figure S1). These data show that the DNA replication process in glioblastoma is blocked by complex **3**.

The annexin V-FITC/propidium iodide (PI) binding assay was used to investigate whether the loss of cancer cell viability promoted by complex **3** is associated with apoptosis. For this purpose, three cell populations, including viable (annexin V-FITC, negative; PI, negative), early apoptotic (annexin V-FITC, positive; PI, negative), and late apoptotic cells or dead cells (annexin V-FITC, positive; PI, positive), were investigated. As the results in Figure 3 show, after 24 h of treatment with complex **3** at 0.3 and 1.0 μM, early (annexin V-FITC, positive; PI, negative) and late apoptosis (annexin V-FITC, positive; PI, positive) takes

dx.doi.org/10.1021/jm101096x | J. Med. Chem. 2011, 54, 5245–5249

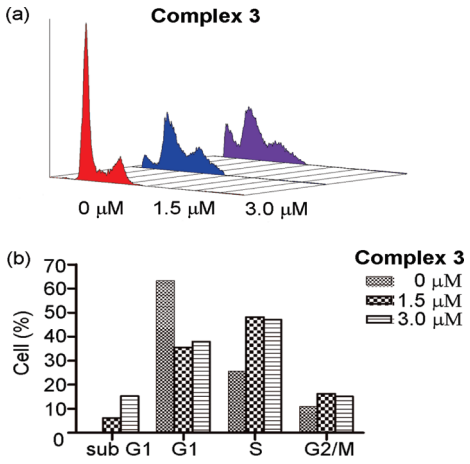

Figure 2. Cell cycle distribution of **3**-treated U-87 MG cells. (a) FACScan analysis of the cell cycle. U-87 MG cells were treated with 1.5 and 3.0 μM **3** for 48 h and then stained with propidium iodide. The cellular DNA content was visualized by using flow cytometry. (b) Graph bars show the distributions at different portions of the cell cycle.

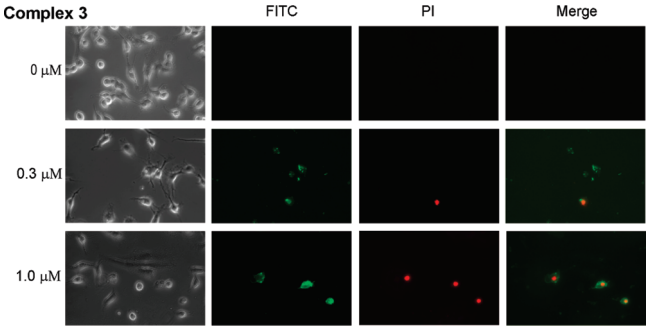

Figure 3. Detection of apoptosis induced by complex **3** in glioblastoma. U-87 MG cells were treated with 0.3 and 1.0 μM **3** for 24 h. Apoptosis was assessed by using fluorescence microscopy analysis of cells labeled with annexin V-FITC/PI.

place with U-87 MG cells, suggesting a proapoptotic activity of complex **3**. This finding is consistent with the observation that treatment of U-87 MG cells with complex **3** induces apoptosis in concert with genomic DNA fragmentation, determined by using agarose gel electrophoresis (Supporting Information Figure S2). Furthermore, the result of a Western blot experiment also demonstrates that **3** causes a dose-dependent increase in protein levels of cleaved caspase-3/cleavage of poly(ADP-ribose)polymerase (cPARP) and a reduction in Bcl-2 levels (Figure 4). Taken together, the results suggest that **3**-induced apoptosis probably follows the intrinsic mitochondrial pathway.

To gain insight into the mode of binding of complex **3** and cisplatin to DNA, UV−vis absorption spectroscopy and gel mobility assays were carried out. The UV−vis absorption spectral analysis of salmon sperm DNA (ssDNA), dosed with cisplatin, shows that a hyperchromic effect with a bathochromic shift slowly arises (Supporting Information Figure S3, parts A and B). Thus, a π-stacking interaction likely occurs between cisplatin and the DNA base pairs.[7a] However, treatment with **3** gives rise to an immediate hyperchromic effect without a bathochromic shift in the UV−vis spectrum of ssDNA (Supporting Information Figure S3, parts C and D). This phenomenon may be a result of the

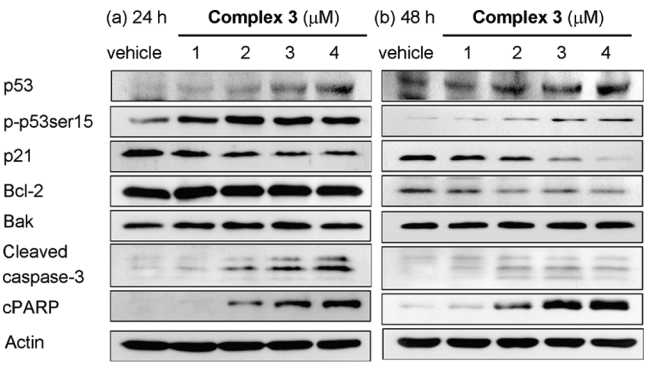

Figure 4. Western blot analysis of the inductive effects of complex **3** on the level of proteins involved in the cell cycle and intrinsic pathway of apoptosis. Experiments were performed in triplicate.

existence of the DNA binding governed by hydrogen bonding or van der Waals interactions.

A gel mobility assay was carried out to determine if movement of ssDNA and pSECTag 2/Hygro B plasmid DNA is altered by applications of increasing concentrations of cisplatin[7b] (Supporting Information Figure S4, parts A and C) and complex **3** (Supporting Information Figure S4, parts B and D). A statistically significant retardation of gel mobility was observed to follow the trend cisplatin > **3**. The absence or decrease in the intensity of the DNA band also followed a similar trend with cisplatin > **3**. These results provide further support that the DNA binding mode of complex **3** is significantly different from that of cisplatin.

Two mechanisms, involving DNA dependent and independent pathways, have been proposed for gold complex mediated apoptosis via mitochondrial pathways.[8a,b] The former route takes place through a major DNA interaction species as the bioactive intermediate, whereas the latter process is promoted by permeability changes of mitochondrial membranes. In vitro antitumor effects of auranofin and related gold(I) complexes are known to be a consequence of their antimitochondrial activities.[8b] Thioredoxin reductases (TrxR), a family of selenoproteins, participate in redox control of the mitochondrial permeability transition and, as a result, are potent targets for antitumor drugs. The results of a number of earlier efforts have demonstrated that auranofin and related gold(I) complexes act as TrxR inhibitors by inducing permeability of mitochondrial membranes and suppressing the growth of cancer cells.[8] To investigate whether the antitumor effects of complex **3** are due to the inhibition of TrxR activity, an assay utilizing a TrxR kit was carried out. The findings show that complex **3** does not inhibit human TrxR at 0.5−4 μM (Supporting Information Figure S5), indicating that **3** does not trigger apoptosis through a DNA independent mechanism.

It is well-known that DNA damage can cause activation of ATM (ataxia telangiectasia mutated) and ATR (ataxia telangiectasia and Rad3-related protein), leading to direct or indirect phosphorylation of a number of cellular proteins (e.g., Chk1, Chk2, p53) involved in the DNA damage response.[9] Chk1 and Chk2 activate p53 activity through phosphorylation and acetylation that results in an increase of mitochondrial membrane permeability and the release of cytochrome *c* during apoptosis. In the studies described above, we determined that complex **3** mediates apoptosis through damage of DNA. Interestingly, the results reveal that ATM, ATR, Chk-1, and Chk-2 (DNA damage-activated protein kinases) are all activated upon treatment with

dx.doi.org/10.1021/jm101096x |*J. Med. Chem.* 2011, 54, 5245–5249

complex **3** under identical conditions (Supporting Information Figure S6). As expected, an accumulation of cleaved caspase-9 and cytosolic cytchrome *c* was observed in response to complex **3**, suggesting that this Au species interacts with DNA in a precarious manner, which in turn initiates operation of a mitochondrial-mediated apoptosis pathway.

In conjunction with these S-phase arrest studies, the effect of complex **3** on cell-cycle-regulating proteins was carried out by using Western blot analysis (Supporting Information Figure S7). It has been shown previously that cyclin D1, in association with cdk4 and cdk6, promotes G1-phase progression and regulates S-phase entry.[10] Expression levels of cdk4, cdk6, and cyclin D1 were either unchanged or slightly decreased upon treatment with complex **3** for 24 and 48 h. Furthermore, the levels of p27 protein, a cyclin-dependent kinase inhibitor that is reduced in the G1−S transition, were found to decrease in a dose-dependent manner. These results suggest that the cells retain the capability of entering the S-phase. Next, we examined whether the levels of other proteins that are required for S-phase progression, including cyclin A, cyclin B1, cyclin E, and cdk2, were also altered by treatment with complex **3**. The findings show that cyclin A and B1 levels remain essentially unchanged after 24 h but that the amounts of both of these proteins decrease in a dose-dependent manner after 48 h (Supporting Information Figure S7). Interestingly, complex **3** treatment causes a decrease of cyclin E and cdk2 expression at 24 and 48 h. Significantly, cdk2 depletion is observed to take place only after 24 h of treatment with the highest concentration (4 μM) of complex **3**. It is clear from the observations made in this effort that complex **3** limits the supply of cyclin A, cyclin B1, and cdk2 and that this phenomenon controls S-phase arrest.

The p53 tumor-suppressor protein, which is induced by DNA damage, is involved in the regulation of cell-cycle arrest or apoptosis.[11] In diverse ways, p53 exerts its effects on the cell cycle by up-regulating the transcription genes encoding p21 and bak that play important roles in the DNA-damage repair process, DNA replication, and apoptosis.[12] To shed light on whether complex **3** activates p53-induced apoptosis in U-87 MG cells, the expression level and phosphorylation status of p53 following treatment by different concentrations of complex **3** for 24 and 48 h were assessed. As the data in Figure 4 show, expression levels of p53, phospho-p53(ser15), and bak are enhanced in a dose-dependent manner. In contrast, p21 in U-87 MG cells is clearly down-regulated by complex **3** (Figure 4). It has been reported earlier that p21 protein levels are typically high in glioma cells and overexpression of p21 may render cells more resistant to p53-mediated apoptosis.[13] Together, these results demonstrate that complex **3** induces apoptosis in U-87 MG cells most likely through a p53-bak pathway that enables p21-mediated apoptotic resistance to be bypassed.

Finally, a control NMR experiment was performed to determine the stability of gold complex **3** in DMSO/PBS solution (9:0.5, PBS = phosphate-buffered saline, pH 7.0)[14] Importantly, this complex was found to be stable in the buffered aqueous solution over a 72 h period at room temperature (Supporting Information Figures S8−S10).[15] This result indicates that intact complex **3** contributes to its in vitro antitumor activity and that an auranofin related species is not responsible for the observed antimitochondrial effect.[16]

CONCLUSION

In an effort focusing on new metal NHC complexes **2**−**4**, we have identified gold complex **3** as a potent anticancer agent, which mediates S-phase arrest via down-regulation of cyclin A, cyclin B1, and cdk2. Apoptosis was induced by this substance in U-87 MG cells through a p53-bak pathway. Of particular interest is that the results show that **3** participates in an important molecular event that mediates negative regulation of p21 and, consequently, that it has therapeutic potential in the treatment of glioblastoma in the case of p21-dependent resistance of p53-induced apoptosis.

EXPERIMENTAL SECTION

Preparation of [[C{(MES)N(CHCH)N($CH_2CH_2NH^tBu$}]Pd-(C_3H_5)]$^+Cl^-$ (2). To a suspension of allyl-Pd-Cl (0.183 g, 0.50 mmol) in 20 mL of THF was added a THF solution of [C{(MES)N-(CHCH)N($CH_2CH_2NH^tBu$}] (**1**)[17] (0.285 g, 1.00 mmol) at room temperature. After the mixture was stirred for 4 h, the precipitate was removed by filtration through Celite. Concentration of the filtrate in vacuo gave a residue, which was crystallized from THF/ether (50:50 volume) at −30 °C to give **2** (0.235 g, 50.0%). Recrystallization of **2** (THF/ether) was carried out twice before biological testing. ^{1}H NMR (C_6D_6, 400 MHz, 25 °C): δ 6.73 (d, $^3J_{H-H}$ = 1.7 Hz, 1H, C*H*), 6.66 (*s*, 2H, C_6H_2), 6.10 (d, $^3J_{H-H}$ = 1.7 Hz, 1H, C*H*), 4.71 (m, 1H, C*H*), 4.37 (m, 2H, CH_2), 4.04 (d, $^3J_{H-H}$ = 7.5 Hz, 2H, CH_2), 2.96 (d, $^3J_{H-H}$ = 13.5 Hz, 2H, CH_2), 2.87 (m, 2H, CH_2), 2.19 (s, 3H, CH_3), 2.09 (s, 6 H, CH_3), 0.94 (s, 9H, ^tBu), 0.78 (s, 1H, NH). ^{13}C NMR ($CDCl_3$, 125 MHz, 25 °C): δ 178.5 ($C_{carbene}$), 139.0 (*Ar*), 136.1 (*Ar*), 135.2 (*Ar*), 128.9 (*Ar*), 122.0 (NCH), 121.8 (NCH), 115.5 (*allyl*), 74.7 (*ally*), 53.2 (*allyl*), 51.5 (NCH_2), 47.2 ($NCMe_3$), 43.9 (NCH_2), 29.2 (CMe_3), 21.0 (Ar-*Me*), 17.9 (Ar-*Me*). HR-MS (FAB): *m*/*z* [(M + H)$^+$] calculated for $C_{21}H_{32}PdClN_3$ 468.6631; found 468.6637.

Preparation of [C{(MES)N(CHCH)N($CH_2CH_2NH^tBu$}]·AuCl (3). To a suspension of AuCl (0.232 mg, 1.00 mmol) in 20 mL of THF was added a THF solution of [C{(MES)N(CHCH)N($CH_2CH_2NH^tBu$}] (**1**) (0.285 g, 1.00 mmol) at room temperature. After the mixture was stirred for 10 min, precipitate was separated by filtration. Concentration of the filtrate in vacuo gave a residue, which was crystallized from THF/toluene (50:50 volume) at −30 °C to give **3** (0.311 g, 60.0%). Recrystallization of **3** (THF/ether) was carried out twice before biological testing. ^{1}H NMR ($CDCl_3$, 500 MHz, 25 °C): δ 7.30 (d, $^3J_{H-H}$ = 1.8 Hz, 1H, C*H*), 6.93 (s, 2H, C_6H_2), 6.81 (d, $^3J_{H-H}$ = 1.7 Hz, 1H, C*H*), 4.28 (t, $^3J_{H-H}$ = 5.8 Hz, 2H, CH_2), 3.05 (t, $^3J_{H-H}$ = 5.5 Hz, 2H, CH_2), 2.30 (s, 3H, CH_3), 1.98 (s, 6 H, CH_3), 1.03 (s, 9H, ^tBu). ^{13}C NMR ($CDCl_3$, 125 MHz, 25 °C): δ 171.6 ($C_{carbene}$), 139.5 (*Ar*), 134.9 (*Ar*), 134.7 (*Ar*), 129.3 (*Ar*), 121.9 (NCH), 121.3 (NCH), 52.8 (NCH_2), 50.5 ($NCMe_3$), 43.3 (NCH_2), 29.0 (CMe_3), 21.0(Ar-*Me*), 17.7 (Ar-*Me*). HR-MS (FAB): *m*/*z* [(M + H)$^+$] calculated for $C_{18}H_{28}AuClN_3$ 518.1637; found 518.1632. Anal. Calcd for $C_{18}H_{27}AuClN_3$: C, 41.75; H, 5.26; N, 8.11. Found: C, 42.04; H, 5.36; N, 8.08.

Preparation of [C{(MES)N(CHCH)N($CH_2CH_2NH^tBu$}]·AgBr (4). A suspension of Ag_2O (0.127 g, 0.55 mmol) and [HC{(MES)N-(CHCH)N($CH_2CH_2NH^tBu$}]Br (0.366 g, 1.00 mmol) in THF (20 mL) was stirred at room temperature overnight. The precipitate was separated by filtration. Concentration of the filtrate in vacuo gave a residue, which was crystallized from THF−toluene (40:60 volume) at room temperature to give **4** (0.420 g, 85%). Recrystallization of **4** (THF/ether) was carried out twice before biological testing. ^{1}H NMR ($CDCl_3$, 500 MHz, 25 °C): δ 7.31 (d, $^3J_{H-H}$ = 1.6 Hz, 1H, C*H*), 6.92 (s, 2H, C_6H_2), 6.87 (d, $^3J_{H-H}$ = 1.7 Hz, 1H, C*H*), 4.21 (t, $^3J_{H-H}$ = 6.0 Hz, 2H, CH_2), 2.95−3.00 (m, 2H, CH_2), 2.30 (s, 3H, CH_3), 1.93 (s, 6 H, CH_3), 1.01 (s, 9H, CMe_3), 0.73 (t, $^3J_{H-H}$ = 8 Hz, 1H, N*H*). ^{13}C NMR ($CDCl_3$, 125 MHz, 25 °C): δ 182.5 ($C_{carbene}$), 139.4 (*Ar*), 135.4 (*Ar*), 134.7 (*Ar*), 129.4 (*Ar*), 122.0 (NCH), 121.9 (NCH), 53.4 (NCH_2), 50.3 ($NCMe_3$), 43.7 (NCH_2), 29.0 ($NCMe_3$), 21.0(Ar-*Me*), 17.6 (Ar-*Me*).

HR-MS (FAB): m/z [(M + H)$^+$] calculated for $C_{18}H_{28}AgBrN_3$ 472.0518; found 472.0516. Anal. Calcd for for $C_{18}H_{28}AgBrN_3$: C, 45.59; H, 5.95; N, 8.86. Found: C, 46.00; H, 5.85; N, 8.81.

■ ASSOCIATED CONTENT

Supporting Information. Experimental details and cellular studies of complex **3** treated U-87 MG cells. This material is available free of charge via the Internet at http://pubs.acs.org.

■ AUTHOR INFORMATION

Corresponding Author

*For T.-G.O.: phone, +886 (2) 27898648; fax, +886 (2) 27831237; e-mail, tgong@chem.sinica.edu.tw. For W.-S.L.: phone, +886 (2) 27898662; fax, +886 (2) 27831237; e-mail, wenshan@chem.sinica.edu.tw.

■ ACKNOWLEDGMENT

We are grateful for financial support provided by the Academia Sinica (Summit Project) and the National Science Council.

■ ABBREVIATIONS USED

NHC, N-heterocyclic carbene; cdk2, cyclin-dependent kinase 2; PS, phosphatidylserine; PARP, poly(ADP-ribose)polymerase; ER, estrogen receptor; BrdU, bromodeoxyuridine; ATM, ataxia telangiectasia mutated; ATR, ataxia telangiectasia and Rad3-related protein; TrxR, thioredoxin reductase

■ REFERENCES

(1) Recent review: Herrmann, W. A. N-Heterocyclic Carbenes: A New Concept in Organometallic Catalysis. *Angew. Chem., Int. Ed.* **2002**, *41*, 1290–1309.

(2) (a) Hickey, J. L.; Ruhayel, R. A.; Barnard, P. J.; Baker, M. V.; Berners-Price, S. J.; Filipovska, A. Mitochondria-Targeted Chemotherapeutics: The Rational Design of Gold(I) N-Heterocyclic Carbene Complexes That Are Selectively Toxic to Cancer Cells and Target Protein Selenols in Preference to Thiols. *J. Am. Chem. Soc.* **2008**, *130*, 12570–12571. (b) Ray, S.; Mohan, R.; Singh, J. K.; Samantaray, M. K.; Shaikh, M. M.; Panda, D.; Ghosh, P. Anticancer and Antimicrobial Metallopharmaceutical Agents Based on Palladium, Gold, and Silver N-Heterocyclic Carbene Complexes. *J. Am. Chem. Soc.* **2007**, *129*, 15042–15053. (c) Cannon, L.; Youngs, W. J. Synthesis, Stability, and Antimicrobial Studies of Electronically Tuned Silver Acetate N-Heterocyclic Carbenes. *J. Med. Chem.* **2008**, *51*, 1577–1583.

(3) (a) Liddle, S. T.; Edworthy, I. S.; Arnold, P. L. Anionic Tethered N-Heterocyclic Carbene Chemistry. *Chem. Soc. Rev.* **2007**, *36*, 1732–1744. (b) Spencer, L. P.; Beddie, C.; Hall, M. B.; Fryzuk, M. D. Synthesis, Reactivity, and DFT Studies of Tantalum Complexes Incorporating Diamido-N-heterocyclic Carbene Ligands. Facile Endocyclic C−H Bond Activation. *J. Am. Chem. Soc.* **2006**, *128*, 12531–12543.

(4) (a) Filipuzzi, S.; Pregosin, P. S.; Albinati, A.; Rizzato, S. Structure, Bonding, and Dynamics of Several Palladium η^3-Allyl Carbene Complexes. *Organometallics* **2008**, *27*, 437–444. (b) Viciu, M. S.; Navarro, O.; Germaneau, R. F.; Kelly, R. A.; Sommer, W.; Marion, N.; Stevens, E. D.; Cavallo, L.; Nolan, S. P. Synthetic and Structural Studies of (NHC)Pd(allyl)Cl Complexes (NHC = N-Heterocyclic Carbene). *Organometallics* **2004**, *23*, 1629–1635.

(5) de Fremont, P.; Scott, N. M.; Stevens, E. D.; Nolan, S. P. Synthesis and Structural Characterization of N-Heterocyclic Carbene Gold(I) Complexes. *Organometallics* **2005**, *24*, 2411–2418.

(6) Teyssot, M. L.; Jarrousse, A. S.; Manin, M.; Chevry, A.; Roche, S.; Norre, F.; Beaudoin, C.; Morel, L.; Boyer, D.; Mahiou, R.; Gautier, A. Metal-NHC Complexes: A Survey of Anti-Cancer Properties. *Dalton Trans.* **2009**, *35*, 6894–6902.

(7) (a) Liu, Z.; Tan, S.; Zu, Y.; Fu, Y.; Meng, R.; Xing, Z. The Interactions of Cisplatin and DNA Studied by Atomic Force Microscopy. *Micron* **2010**, *41*, 833–839. (b) Farhad, M.; Yu, J. Q.; Beale, P.; Fisher, K.; Huq, F. Studies on the Synthesis and Activity of Three Tripalladium Complexes Containing Planaramine Ligands. *ChemMedChem* **2009**, *4*, 1841–1849.

(8) (a) Galluzzi, L.; Larochette, N.; Zamzami, N.; Kroemer, G. Mitochondria as Therapeutic Targets for Cancer Chemotherapy. *Oncogene* **2006**, *25*, 4812–4830. (b) McKeage, M. J. Gold Opens Mitochondrial Pathways to Apoptosis. *Br. J. Pharmacol.* **2002**, *136*, 1081–1082. (c) Ott, I.; Qian, X.; Xu, Y.; Vlecken, D. H.; Marques, I. J.; Kubutat, D.; Will, J.; Sheldrick, W. S.; Jesse, P.; Prokop, A.; Bagowski, C. P. A Gold(I) Phosphine Complex Containing a Naphthalimide Ligand Functions as a TrxR Inhibiting Antiproliferative Agent and Angiogenesis Inhibitor. *J. Med. Chem.* **2009**, *52*, 763–770. (d) Cox, A. G.; Brown, K. K.; Arner, E. S.; Hampton, M. B. The Thioredoxin Reductase Inhibitor Auranofin Triggers Apoptosis through a Bax/Bak-Dependent Process That Involves Peroxiredoxin 3 Oxidation. *Biochem. Pharmacol.* **2008**, *76*, 1097–1109.

(9) (a) Shiloh, Y. ATM and ATR: Networking Cellular Responses to DNA Damage. *Curr. Opin. Genet. Dev.* **2001**, *11*, 71–77. (b) Helt, C. E.; Cliby, W. A.; Keng, P. C.; Bambara, R. A.; O'Reilly, M. A. Ataxia Telangiectasia Mutated (ATM) and ATM and Rad3-Related Protein Exhibit Selective Target Specificities in Response to Different Forms of DNA Damage. *J. Biol. Chem.* **2005**, *280*, 1186–1192.

(10) Sherr, C. J. Cancer Cell Cycles. *Science* **1996**, *274*, 1672–1677.

(11) (a) Bitomsky, N.; Hofmann, T. G. Apoptosis and Autophagy: Regulation of Apoptosis by DNA Damage Signalling—Roles of p53, p73 and HIPK2. *FEBS J.* **2009**, *276*, 6074–6083. (b) Amano, T.; Nakamizo, A.; Mishra, S. K.; Gumin, J.; Shinojima, N.; Sawaya, R.; Lang, F. F. Simultaneous Phosphorylation of p53 at Serine 15 and 20 Induces Apoptosis in Human Glioma Cells by Increasing Expression of Pro-Apoptotic Genes. *J. Neuro-Oncol.* **2009**, *92*, 357–371. (c) Vogelstein, B.; Lane, D.; Levine, A. J. Surfing the p53 Network. *Nature* **2000**, *408*, 307–310.

(12) (a) Qin, J.; Chen, H. G.; Yan, Q.; Deng, M.; Liu, J.; Doerge, S.; Ma, W.; Dong, Z.; Li, D. W. Protein Phosphatase-2A Is a Target of Epigallocatechin-3-Gallate and Modulates p53-Bak Apoptotic Pathway. *Cancer Res.* **2008**, *68*, 4150–4162. (b) Norbury, C. J.; Zhivotovsky, B. DNA Damage-Induced Apoptosis. *Oncogene* **2004**, *23*, 2797–2808.

(13) (a) Gomez-Manzano, C.; Fueyo, J.; Kyritsis, A. P.; McDonnell, T. J.; Steck, P. A.; Levin, V. A.; Yung, W. K. Characterization of p53 and p21 Functional Interactions in Glioma Cells en Route to Apoptosis. *J. Natl. Cancer Inst.* **1997**, *89*, 1036–1043. (b) Jung, J. M.; Bruner, J. M.; Ruan, S.; Langford, L. A.; Kyritsis, A. P.; Kobayashi, T.; Levin, V. A.; Zhang, W. Increased Levels of p21WAF1/Cip1 in Human Brain Tumors. *Oncogene* **1995**, *11*, 2021–2028. (c) Wang, J.; Walsh, K. Resistance to Apoptosis Conferred by Cdk Inhibitors during Myocyte Differentiation. *Science* **1996**, *273*, 359–361.

(14) See Supporting Information for more details.

(15) We also performed a similar control experiment for complex **2** and **4**. Upon dissolution of these complexes in the buffer solution, we observed a rapid and irreversible decomposition of the species under physiologically relevant conditions, suggesting that effective biological functions were achieved by a prodrug of complex **2** or **4**.

(16) (a) Gromer, S.; Arscott, L. D.; Williams, C. H.; Schirmer, R. H.; Becker, K. Human Placenta Thioredoxin Reductase. Isolation of the Selenoenzyme, Steady State Kinetics, and Inhibition by Therapeutic Gold Compounds. *J. Biol. Chem.* **1998**, *273*, 20096–200101. (b) Barnard, P. J.; Berners-Price, S. J. Targeting the Mitochondrial Cell Death Pathway with Gold Compounds. *Coord. Chem. Rev.* **2007**, *251*, 1889–1902.

(17) Shih, W.-C.; Wang, C.-H.; Chang, Y.-T.; Yap, G. P. A.; Ong, T.-G. Synthesis and Structure of an Amino-Linked N-Heterocyclic Carbene and the Reactivity of Its Aluminum Adduct. *Organometallics* **2009**, *28*, 1060–1067.